Removal of Methylene Blue from Aqueous Solution Using *Typha* Stems and Leaves

Raymundo Sánchez-Orozco,[a,*] Miriam Martínez-Juan,[a] José Juan García-Sánchez,[a] and Fernando Ureña-Núñez [b]

The aim of this study was to investigate the potential of *Typha latifolia* L. stem and leaf powder (T-SLP) to remove methylene blue (MB), a cationic dye, from aqueous solutions. The T-SLP was used without any modification. The batch adsorption experiments were carried out at 25 °C under varying operating parameters, namely pH, initial concentration, contact time, and adsorbent dose. Equilibrium isotherms and kinetics were used for data analysis. The surface morphology of the adsorbent and the possible interactions between the T-SLP and MB were characterized by scanning electron microscopy (SEM) and Fourier transform infrared spectroscopy (FT-IR), respectively. The experimental data fitted well to the Langmuir model, with a maximum adsorption capacity of 126.6 mg g^{-1}. The efficiency of dye removal in the substrate was high, reaching a maximum value of 98.69%. Intra-particle diffusion was involved in the adsorption process, and the pseudo-second-order kinetics was the best fit for the adsorption of MB onto T-SLP, with a high correlation ($R^2 \geq 0.9993$) for all initial MB concentrations studied. The results of this work revealed that T-SLP can be used as a potential alternative for the rapid removal of MB from aqueous solutions.

Keywords: Typha latifolia; Methylene blue; Equilibrium; Adsorption isotherms; Kinetics

*Contact information: a: Tecnológico de Estudios Superiores de Jocotitlán, Carretera Toluca-Atlacomulco Km 44.8, Ejido San Juan y San Agustín, C. P. 50700 Jocotitlán, Estado de México, México; b: Instituto Nacional de Investigaciones Nucleares, Apartado Postal 18-1027, Col. Escandón, C. P. 11801 Ciudad de México, México; *Corresponding author: r.sanchez@tesjo.edu.mx*

INTRODUCTION

The removal of hazardous compounds from industrial effluents is one of the most serious environmental challenges in recent years. Synthetic dyes are widely used in the textile, paper, leather, plastic, printing, and cosmetic industries (Saif *et al*. 2012; Anisuzzaman *et al*. 2015; Peydayesh and Rahbar-Kelishami 2015). Effluents with small amounts of dye can cause local environmental problems and at the same time might significantly affect photosynthetic aquatic life by reducing the transmission of sunlight. Because of their synthetic and toxic nature, dyes have a severe impact on human health, causing many problems, such as allergies, dermatitis, skin irritation, cancer, and mutations (Nasuha and Hameed 2011; Gouamid *et al*. 2013).

To remediate polluted water, various treatment processes have been studied for dye removal, including physicochemical/biological treatment technologies (Dutta *et al*. 2011; Hubbe *et al*. 2012). Among them, adsorption is considered a promising technique because of its flexibility, simplicity of design, ease of operation, high efficiency, and low cost in comparison with other methods (de Lima *et al*. 2012; Guo *et al*. 2014). Recently, an extensive array of adsorbents for the removal of dyes from aqueous solutions has been

investigated. These include palm ash, bamboo dust, orange peel, sugarcane bagasse, tealeaves, *Luffa cylindrica* fibers, rice husk, water hyacinth, and other waste materials (Hameed 2009; Saif *et al*. 2012; Esan *et al*. 2014).

The cattail (*Typha latifolia* L.) is an invasive plant, with currently no economic value, that has shown potential as an adsorbent for the removal of dye from synthetic wastewater. Previous studies have shown that aquatic weeds such as cattails can act as phytoremediators of contaminants in aqueous media (Saif Ur Rehman and Han 2013; Rodriguez-Hernandez *et al*. 2017). This aquatic plant offers a large amount of biomass composed primarily of cellulose, hemicelluloses, and lignin that can be used for adsorption purposes (Kumari and Tripathi 2015; Rebaque *et al*. 2017). It has been commonly used in constructed wetlands as an effective alternative for the treatment of septic effluents (Meng *et al*. 2016).

There are several studies that have used cattail biomass in different forms to remove contaminants from aqueous solutions. In such work, Lu and Liang (2013) used acid modification of *Typha angustifolia*, Hu *et al*. (2010) used cattail root to remove Congo Red, Shi *et al*. (2010) have reported the preparation of active carbon for dye removal, Kumari and Tripathi (2015) demonstrated the removal of heavy metals, and Rodriguez-Hernandez *et al*. (2017) employed *Typha angustifolia* as a potential phytoremediator of 2,4-dichlorophenol. It is well known that *Typha latifolia* is a hyperaccumulator emergent plant. Moreover, it can be used as a low-cost sorbent by considering its highly porous structure to treat wastewater (Saif Ur Rehman and Han 2013). It has been demonstrated that the sorption properties of cattail are due to the presence of functional groups, such as carboxylic, hydroxyl, and phenols, which have an affinity for a wide range of pollutants (Xu *et al*. 2011). Therefore, this research focuses on exploring the potential of *Typha latifolia* stem and leaf powder for the removal of methylene blue from synthetic solutions through batch studies. The influence of different parameters, such as contact time, initial dye concentration, dosage absorbent, and pH, on the adsorption was investigated. For validation of the experimental data, the adsorption equilibriums, isotherms, and kinetics parameters were also evaluated.

EXPERIMENTAL

Materials

The cattail plants (*Typha latifolia* L.) used in this study were collected from a lagoon in Tiacaque Village, Jocotitlan, Mexico. The stems and leaves of the cattail were cut into small pieces, washed several times with distilled water to remove any adhering dirt, and then dried in an oven at 65 °C until a constant mass was obtained. After drying, this material was ground in a domestic grinder and sieved to obtain particles of approximate size between 0.5 and 1.0 mm. Finally, the resulting powder constituted by the mixture of stem and leaf was stored in a plastic bottle for further use in adsorption experiments. No additional physico-chemical treatment was applied to the biomass.

Methods

Preparation of adsorbate

Methylene blue ($C_{16}H_{18}N_3Cl{\cdot}3H_2O$) MB was purchased from a local supplier and used without further purification. The MB stock solution was prepared by dissolving 0.5 g of dye in distilled water in a 1000-mL volumetric flask to a concentration of 0.5 g L^{-1}. The

experimental solutions were obtained by diluting the dye stock solution to the needed initial concentrations, ranging from 50 to 300 mg L^{-1}. Additionally, a series of standard solutions were prepared in the concentration range of 0 to 12 mg L^{-1} by successive dilutions to obtain the calibration curve for the determination of the dye concentration of unknown solutions.

Adsorption experiments

Batch adsorption studies of MB onto cattail were carried out in 150 mL stoppered Erlenmeyer flasks with 50 mL of MB solution with a concentration of 100 mg L^{-1}. A fixed amount of 0.1 g of adsorbent was accurately weighed and added to the solution. The glass Erlenmeyer flasks were capped and agitated mechanically at 200 rpm using a rotary shaker for 180 min at room temperature (25 °C). The influences of various adsorbent doses, initial pH values, contact times, and initial dye concentrations were studied. The effect of adsorbent dosage was varied from 0.025 to 0.3 g. The range of the initial pH values of MB aqueous solutions was 2 to 10, adjusted by aliquots of 0.1 M NaOH and 0.1 M HCl using a pH meter (Thermo Fisher Scientific Inc., Waltham, MA). The contact time on the adsorption process was varied from 0 to 180 min. The initial dye concentrations used were 50, 100, 150, 200, 250, and 300 mg L^{-1}. In each case, after the process was completed, samples were collected from the flasks at predetermined time intervals, and then dye solutions were separated from the adsorbent by centrifugation at 4500 rpm for 15 min. After being centrifuged, supernatant liquids were analyzed for the determination of the final concentration of MB using a Genesys 10S UV–vis spectrophotometer (Thermo Scientific) with 665 nm (Guo *et al*. 2014) as the maximum absorbance wavelength. All the experiments were performed in triplicate, and the average values were considered.

The amount of dye adsorbed at time t (q_t) and at equilibrium time (q_e) and the dye removal percentage were calculated using Eqs. 1, 2, and 3, respectively:

$$q_t = \frac{(C_o - C_t)V}{M} \quad (1)$$

$$q_e = \frac{(C_o - C_e)V}{M} \quad (2)$$

$$\%\, Removal = \frac{C_o - C_e}{C_o} \times 100 \quad (3)$$

where C_o and C_t (mg/L) are the initial and final concentrations of MB, respectively; C_e (mg/L) is the concentration of dye at equilibrium time; M (g) is the mass of adsorbent used; and V (L) is the volume of dye solution.

Adsorbent characterization

The possible changes in surface morphology of the absorbent were observed by scanning electron microscopy (SEM; JEOL JSM-IT100, Japan). The SEM samples were prepared by depositing the particles homogeneously on a conductive adhesive carbon tape. The specimens were imaged under a low vacuum at 15 kV using the back-scattered electron detector. An FTIR study was performed using an FTIR spectrophotometer with a UATR sampling accessory (Perkin Elmer Spectrum Two, USA) to identify functional groups present on the adsorbent samples before and after the adsorption process. The spectra were recorded in the range of 4000 to 500 cm^{-1}.

Adsorption isotherms studies

The adsorption equilibrium data are generally expressed as adsorption isotherms. This describes the nature of the adsorbent-adsorbate and their mutual interaction on the adsorption process (Gouamid *et al*. 2013). In this work, three parametric models, Langmuir, Freundlich, and Temkin, were employed to investigate the adsorption behaviour. The Langmuir isotherm, which has been commonly used for sorption processes, can be applied to explain the adsorption of MB onto T-SLP. This adsorption model is based on the assumption that the monolayer adsorption occurs on a completely homogeneous surface of the adsorbent and can be represented by the following expression (Zhou *et al*. 2011; Anisuzzaman *et al*. 2015),

$$\frac{C_e}{q_e} = \frac{1}{q_{max} K_L} + \frac{C_e}{q_{max}} \quad (4)$$

where q_e and q_{max} (mg·g^{-1}) are the adsorption capacity at equilibrium and the theoretical maximum adsorption capacity, respectively; C_e (mg L^{-1}) is the concentration of MB solution at equilibrium; and K_L is a constant related to the adsorption energy (L·mg^{-1}). The values of K_L and q_{max} are calculated from the slope and intercept of the linear plot of C_e/q_e *versus* C_e. The essential characteristics of a Langmuir isotherm can be expressed in terms of a dimensionless constant separation factor R_L that is defined by,

$$R_L = \frac{1}{1 + K_L C_o} \quad (5)$$

where C_o is the highest initial dye concentration (mg L^{-1}), and R_L indicate the tendency of the isotherm to be either unfavorable ($R_L > 1$), linear ($R_L=1$), favorable ($0 < R_L < 1$), or irreversible ($R_L=0$) (Nasuha and Hameed 2011). The R_L values between 0 and 1 represent favorable adsorption.

Different from the Langmuir, the Freundlich isotherm is an empirical equation that assumes that the non-ideal adsorption occurs on heterogeneous surfaces with a non-uniform distribution of energy levels and describes a reversible adsorption, with no restriction on the formation of a monolayer. The Freundlich equation (Chowdhury *et al*. 2011; Irem *et al*. 2013; Esan *et al*. 2014) is given by,

$$\ln q_e = \ln K_F + \frac{1}{n} \ln C_e \quad (6)$$

where K_F (mg g^{-1} (L mg^{-1})$^{1/n}$) is the Freundlich constant, which is a measure of the adsorption capacity of the adsorbent, and *n* is an empirical constant which gives valuable information about the isotherm shape. The magnitude of the exponent, *1/n*, gives an indication of the favorability of the adsorption process. Values of $n > 1$ represent a favorable adsorption condition. Using equation (6), a plot of ln q_e *versus* ln C_e will give a straight line with slope of *1/n* and intercept of ln K_F.

On the other hand, the Temkin isotherm is based on the assumption that the heat of adsorption would decrease linearly with coverage of the adsorbent. The equation of the Temkin isotherm (Hameed 2009; Hameed and Ahmad 2009; Shakoor and Nasar 2016) is represented in the following form,

$$q_e = \frac{RT}{b_T} \ln K_T \; \frac{RT}{b_T} \ln C_e \quad (7)$$

where R (8.314 J mol^{-1} K^{-1}) is gas universal constant, T (K) is the absolute temperature, b_T is a constant related to adsorption heat (J mol^{-1}), and K_T (L g^{-1}) is the constant corresponding to maximum binding energy. The values of b_T and K_T were calculated from the slopes and intercepts of q_e *versus* ln C_e.

Adsorption kinetics

Kinetic models were used to determine the sorption mechanism of MB onto T-SLP as function of time. The kinetic models considered were the pseudo-first-order equation, the pseudo-second-order equation, and the intraparticle diffusion.

The pseudo-first-order rate equation is generally expressed by Eq. 8 (Lagergren 1898). The pseudo-second-order model (Ho and McKay 1999) was also used to explain the sorption kinetics and can be expressed by Eq. 9,

$$\ln (q_e - q_t) = \ln q_e - k_1 t \quad (8)$$

$$\frac{t}{q_t} = \frac{1}{k_2 \cdot q_e^2} + \frac{t}{q_e} \quad (9)$$

where q_e and q_t (mg g^{-1}) are the amount of MB adsorbed at equilibrium and at any time t (min), respectively, k_1 (min^{-1}) is the rate constant of pseudo-first-order adsorption, and k_2 (g mg^{-1} min^{-1}) is the specific rate constant of pseudo-second-order adsorption. The values of k_1 and q_e are acquired from the slope and intercept of the plot of ln (q_e –q_t) *versus t*, respectively. Similarly, k_2 and q_e are calculated from the intercept and slope through plotting t/q_e *versus t*.

The intra-particle diffusion model (Weber and Morris 1963) was also applied to investigate any possible role of diffusion in the mechanism of MB adsorption on T-SLP by using the empirical Eq. 10,

$$q_t = k_{id} \cdot t^{1/2} + C \quad (10)$$

where k_{id} (mg g^{-1} min$^{-1/2}$) is the intra-particle rate of diffusion and C (mg g^{-1}) is the boundary layer thickness. The plot of q_t *versus* $t^{1/2}$ gives a straight line with slope K_{id} and intercept C. If the lines pass through the origin, the intraparticle diffusion is involved in the adsorption process, and therefore the intraparticle diffusion is the rate-controlling step. However, if the data exhibit plots with multimodal regions, then the process is governed by two or more steps (Gouamid *et al*. 2013; Irem *et al*. 2013).

RESULTS AND DISCUSSION

Characterization of Adsorbent Samples

FTIR analysis of MB adsorption onto T-SLP

The FTIR spectra of T-SLP were used to analyze the functional groups before and after the adsorption of the MB. The broad absorption peak at 3339 cm^{-1}, seen in Fig. 1, was attributed to the stretching vibrations of the O-H groups of the cellulosic structure of the T-SLP, thus showing the existence of free hydroxyl groups on the T-SLP surface. Therefore, the peak appearing at 2918 cm^{-1} was evidence of the alkyl stretch vibrations of the C-H bond that was associated with the presence of -CH_3. The peak appearing at 1731 cm^{-1} was assigned to the C=O stretching vibrations of the aldehydes and ketones. Meanwhile, the stretching vibration at 1604 cm^{-1} was related to the conjugate C=C bond

of alkenes, *i.e*., the characteristics of cellulose and hemicellulose (Peydayesh and Rahbar-Kelishami 2015; Etim *et al*. 2016). The peak located at 1331 cm^{-1} was assigned to the stretch vibration of C–O from the carboxyl group. On the other hand, the intense and predominant peak around 1035 cm^{-1} was assigned to the C–O–C functional group of the cellulose and lignin structures of T-SLP. The changes observed in the FTIR spectrum reflects the evidence for the interaction between MB molecules and the functional groups present on the surface of the T-SLP that might be involved in the adsorption process of the dye. Moreover, it could be seen that there was no real shift in the absolute values of the absorption peaks, but the intensity became higher after absorption, which indicated a physical adsorption. Similar observations have been reported by other works (Guo *et al*. 2014; Shakoor and Nasar 2016).

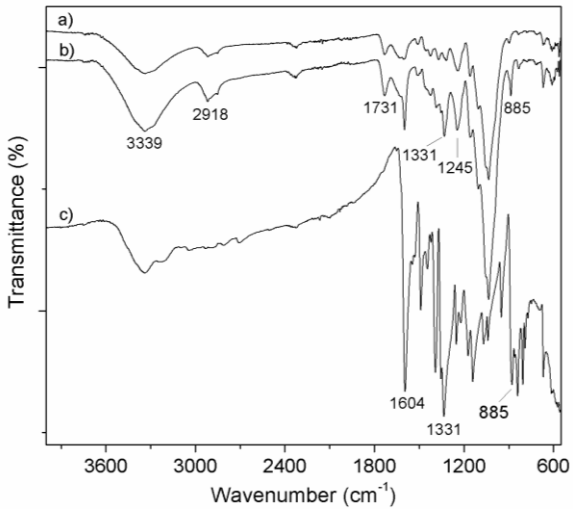

Fig. 1. FTIR spectra of a) T-SLP before adsorption process, b) T-SLP adsorbed with MB and c) methylene blue dye

Scanning electron microscopy of adsorbent

The surface of the *T. latifolia* before and after the adsorption experiments was studied using SEM. As shown in Fig. 2, the micrograph of the biosorbent exhibited a heterogeneous morphology with some cavities and exposure of the cell wall structure of the fibers. Additionally, it was possible to observe significant fracturing and sectioning of the cell wall due to the grinding process. These disruptions are useful for the dye adsorption because they provide suitable binding sites and ready access to the small surface area for the sorption process, and, consequently, most of the pores could be covered by dye molecules.

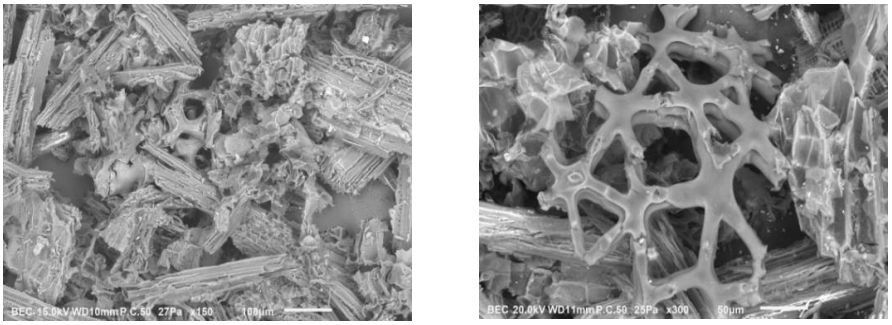

Fig. 2. Scanning electron micrographs (SEM): a) T-SLP before adsorption process and b) T-SLP adsorbed with MB

Effect of Adsorbent Dose

The dosage of the biomass is an important factor to consider in the efficiency of adsorption dyes. As shown in Fig. 3, the adsorption of MB increased significantly from 31.0% to 98.7% with the increase in the amount of T-SLP added from 0.0125 to 0.3 g. A further increase in the adsorbent dosage beyond 0.15 g did not have a remarkable effect on the adsorption capacity, after which equilibrium was attained. These results can be explained by the fact that the surface area of the adsorbent increased, and there were more available adsorption sites for the sorbent-solute interaction as a result of the increase in the adsorbent dose. It should be noted that if the adsorption capacity is expressed in mg g^{-1} of biomass, the capacity decreases with the increase in the amount of adsorbent. This can be attributed to the overlap or aggregation of the adsorption sites, as a consequence of an increase in the total adsorption surface available for the dye and an increase in the diffusion path length (Chowdhury *et al*. 2011; Etim *et al*. 2016).

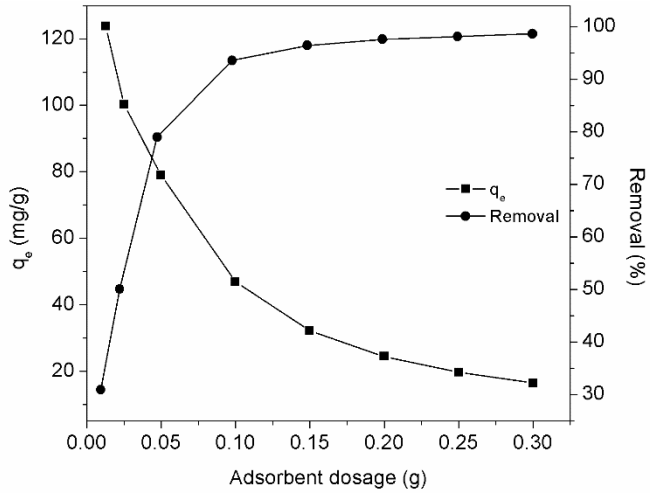

Fig. 3. Effect of adsorbent dosage on T-SLP adsorption; initial concentration: 100 mg L^{-1}, contact time: 180 min, agitation speed: 200 rpm, room temperature: 25±1 °C

Effect of Initial pH

The initial pH of the dye solution is one of the most important parameters involved in batch adsorption systems and particularly for the adsorption capacity; it influences the magnitude of electrostatic charges that are imparted both by the ionized dye molecules and by the surface charge of the solid adsorbent (Esan *et al*. 2014; Shakoor and Nasar 2016). The results in Fig. 4 exhibit a sharp increment in the adsorption capacity as the pH was increased from 2.0 to 6.0. However, the difference in the removal percentage did not change significantly with further increase in pH from 6 to 10, and the decolorization efficiency was almost constant. The lowest removal was obtained at pH 2 (32.7%), while the best adsorption was at pH 10 (97.9%). It can be seen that the pH of the solution had a notable effect on the amount of MB adsorbed. When the pH of the dye solution increased, the surface of the T-SLP acquired a negative charge, resulting in increased adsorption of the MB due to an increase in the electrostatic attraction between the negatively charged adsorbent and the positively charged dye. Hence, at higher pH the negative charged groups (carboxyl and hydroxyl groups) became increasingly ionized, thus resulting in more negative charge of the sorbent surface, leading to maximum adsorption of MB (AlOthman *et al*. 2014). On the other hand, the lower adsorption of MB in the acidic medium (lower pH) could be attributed to the excess of H^+ ions in solution competing with the dye cations

for adsorption sites. Therefore, the results suggested that the removal efficiency was favored in alkaline environment over acidic conditions. Similar phenomena were also reported for the adsorption of methylene blue on garlic peel (Hameed and Ahmad 2009), pineapple waste (Hameed *et al*. 2009), banana stalk waste (Hameed *et al*. 2008b), and bamboo (Guo *et al*. 2014).

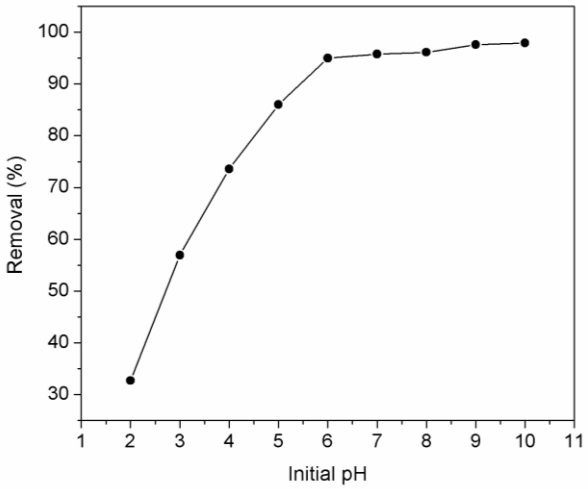

Fig. 4. Effect of pH on the percent removal of MB by T-SLP; initial concentration: 100 mg L^{-1}, contact time: 180 min, agitation speed: 200 rpm, room temperature: 25±1 °C

Effect of Contact Time and Initial Dye Concentration

Figure 5 shows the effect of contact time and initial dye concentration on the adsorption of MB onto T-SLP. As observed, the amount of MB adsorbed increased sharply for the first 10 min, followed by a slower rate of adsorption between 10 and 60 min, until finally the equilibrium was reached. The drastic increase in adsorption capacity during the initial contact time may be attributed to the availability of vacant sites on the surface of T-SLP, whereas in the later stage of the adsorption the increase became more gradual because of the diffusion of dye in the pores of the adsorbent because the external sites were completely occupied.

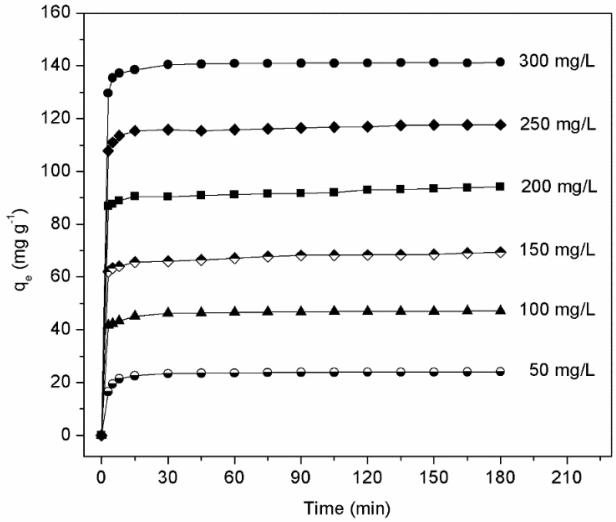

Fig. 5. Effect of initial dye concentration and contact time on the adsorption of T-SLP; dosage: 0.1 g, pH: 7, stirring speed: 200 rpm and room temperature: 25±1 °C

As can be seen from Fig. 5, the equilibrium adsorption increased from 24.1 to 141.3 mg g^{-1}, with an increase in the initial MB concentration from 50 to 300 mg L^{-1}. The results showed that the time required for the adsorbent to reach equilibrium was about 60 min. However, experimental measurements of the data were obtained at 180 min to be sure that full equilibrium was attained. The study assumed that the initial concentration was not having any significant effect on the contact time to reach equilibrium. In addition, the time required to reach equilibrium was faster compared to other adsorbents, which generally required a contact time of more than 120 minutes (Hameed and Ahmad 2009; Hameed *et al*. 2009). Therefore, the rapid uptake of adsorbate by an adsorbent is very important when the adsorption is applied in the treatment of wastewater containing dyes.

Adsorption Isotherms Studies

An adsorption isotherm describes the interaction behavior between adsorbent and adsorbate at a constant temperature. It also offers explanation for the nature, surface properties, affinity of the adsorbent, as well as the mechanism of the adsorption process (Zhou *et al*. 2011). The experimental data obtained in the present study were fitted to different absorption isotherms. The parameters and correlation coefficients obtained from the plots of Langmuir (C_e/q_e versus C_e), Freundlich (ln q_e versus ln C_e), and Temkin (q_e versus ln C_e) relationships (figures not shown) are listed in Table 1. The value of R^2 obtained from the Langmuir isotherm equation (0.9967) was statistically significant and fit the data better than the Freundlich (0.9765) and Tempkin (0.9827) isotherm equations, reflecting the fact that the adsorption of MB onto T-SLP takes place as monolayer coverage on a surface that is evenly distributed. Besides the value of R^2, the standard deviation (*SD*) were obtained to determine the validity of the models and to reproduce experimental data. It can also be observed from Table 1 that the calculated maximum monolayer adsorption capacity (q_{max}) of T-SLP for MB was relatively large, at 126.6 mg g^{-1}.

Table 1. Constant Parameters of Isotherm Models for MB Adsorption onto T-SLP

Isotherm	Parameters
Langmuir	
q_m (mg g^{-1})	126.6
K_L (L mg^{-1})	0.0942
R^2	0.9967
SD	1.1245
Freundlich	
K_F (mg g^{-1}(L $mg^{-1})^{1/n}$)	15.6269
n	1.9968
R^2	0.9765
SD	3.3146
Temkin	
A (L g^{-1})	1.1579
B	24.8370
R^2	0.9827
SD	2.1680

To evaluate the ability of the different isotherm models to correlate the experimental equilibrium data, the predicted non-linear plots were compared with the experimental results for the adsorption of MB onto T-SLP. From Fig. 6a, it can be seen that the isotherm curves showed the superposition of the experimental and theoretical

results. The relationships between R_L and initial MB concentrations are shown in Fig. 6b, in which it can be observed that the value of R_L decreased with the increase in initial MB concentration. The R_L values obtained in this study were smaller than 1.0, indicating the high affinity of MB to T_L and that the adsorption was more favorable at higher concentrations.

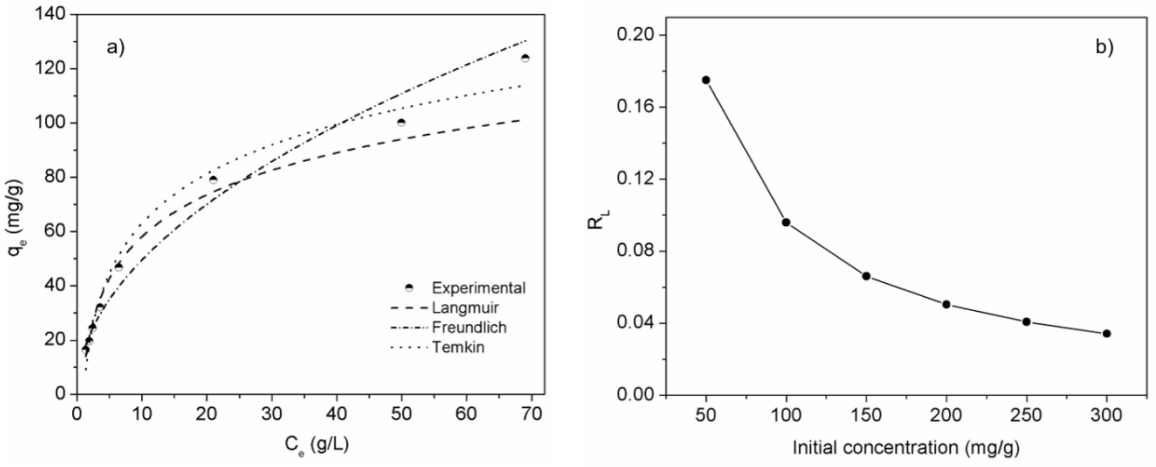

Fig. 6. a) Experimental data compared with modeled isotherms profiles for adsorption of MB by T-SLP; b) Separation factor for adsorption of MB by T-SLP

In addition, Table 2 shows the comparison of the adsorption capacity of T-SLP with other adsorbents for the MB adsorption reported in previous works. It should be considered that in all cases, the adsorption was under different experimental conditions, and therefore the removal capacity was not comparable. Despite this, the value of q_{max} obtained is in the range of the adsorption capacity of most adsorbents, and may be in competition with some commercial type adsorbents. Based on that, it was obvious that the experimental results showed a great potential towards the application of T-SLP in the removal of dyes present in effluents.

Table 2. Comparison of Maximum Adsorption of Methylene Blue on Different Adsorbents without any Chemical Treatment

Adsorbent	q_{max} (mg g^{-1})	Reference
Typha latifolia stems and leaves	126.6	This research
Platanus orientalis leaves	114.9	(Peydayesh & Rahbar-Kelishami 2015)
Broad bean peels	192.7	(Hameed and El-khaiary 2008)
Typha angustata phytomass	8.01	(Saif Ur Rehman and Han 2013)
Coconut bunch waste	70.9	(Hameed *et al*. 2008a)
Orange waste	30.3	(Irem *et al*. 2013)
Spent corncob	121.3	(Zhou *et al*. 2011)
Durian skin	7.23	(Anisuzzaman *et al*. 2015)
Citrus limetta peel	227.3	(Shakoor and Nasar 2016)
Luffa cylindrical sponge	18.2	(Esan *et al*. 2014)
Date palm leaves	58.1	(Gouamid *et al*. 2013)
Pineapple stem	119.0	(Hameed *et al*. 2009)
Spent rice	8.13	(Saif *et al*. 2012)
Citrus fruit peel	25.5	(Dutta *et al*. 2011)

Kinetics studies

The data obtained from the contact time dependent experiments were used to evaluate the kinetics of the adsorption process. This implies predicting the adsorption rate and the search for a model that adequately fitted the experimental data as a function of several operating conditions. In the present study, the data for the adsorption of the MB dye onto T-SLP were analyzed by applying the pseudo-first-order, pseudo-second-order, and intraparticle diffusion models at initial concentrations of 50 to 300 mg L^{-1}. The kinetic parameters for the adsorption of MB onto T-SLP are given in Tables 3 and 4. The values of $q_{e,cal}$ obtained from the pseudo-second-order model were closer to the experimental results than were the $q_{e,cal}$ obtained from Lagergren's pseudo-first-order model (Table 3). This was also evident in the higher values of the adsorption rate constant (k_1) when compared to the (k_2) values in the pseudo-second-order model, which showed the deviation between the experimental results and the calculated values for the adsorption of MB onto T-SLP. The values of k_{id} and C from the intraparticle diffusion model were also calculated. From Table 4, it can be observed that the values of C increased from 23.0 to 138.6 mg g^{-1} with an increase in the initial dye concentration from 50 to 300 mg L^{-1}, which indicated an increase in the thickness and the effect of the boundary thickness (Anisuzzaman *et al*. 2015). Similar results have been reported for the adsorption of MB onto palm waste (AlOthman *et al*. 2014) and orange waste (Irem *et al*. 2013).

Table 3. Constant Parameters of Various Kinetic Models for the Adsorption of MB on T-SLP

C_o	$q_{e,exp}$	Pseudo-first-order Model			Pseudo-second-order Model		
(mg L^{-1})	(mg g^{-1})	$q_{e,cal}$ (mg g^{-1})	k_1 (min^{-1})	R^2	$q_{e,cal}$ (mg g^{-1})	k_2 (mg g^{-1} min^{-1})	R^2
50	24.04235	1.0234	0.00698	0.98363	24.1196	6.12363×10^{-5}	0.99998
100	47.10915	1.2925	0.00779	0.96824	47.2589	1.52293×10^{-5}	0.99999
150	69.30537	1.9913	0.00590	0.96008	69.7836	5.55458×10^{-5}	0.99983
200	94.12125	2.3487	0.00510	0.75920	94.1619	8.45375×10^{-5}	0.99930
250	117.66675	1.7917	0.00655	0.98360	118.2033	1.32041×10^{-5}	0.99997
300	141.38059	1.3818	0.00649	0.75380	141.4427	3.97023×10^{-6}	1.00000

Table 4. Intraparticle Diffusion Constants for Various Initial MB Concentrations at 25 °C

C_o (mg L^{-1})	$q_{e,exp}$ (mg g^{-1})	C (mg g^{-1})	k_{id} (mg g^{-1} $min^{-1/2}$)	R^2
50	24.04235	22.98141	0.08069	0.96985
100	47.10915	45.09968	0.16151	0.80347
150	69.30537	63.78218	0.41945	0.94901
200	94.12125	87.11771	0.46136	0.85510
250	117.66675	113.84800	0.28258	0.98430
300	141.38059	138.63150	0.22145	0.73310

By comparing Figs. 7a and 7b, it is obvious that the pseudo-second-order model fit the experimental data better than pseudo-first-order model for the entire adsorption period. The coefficient of determination R^2 values of the pseudo-second-order model (0.9993 to 1.0) were found to be higher than the R^2 values obtained for the pseudo-first-order model (0.75385 to 0.98363). Therefore, it could be concluded that the pseudo-second-order kinetic model provided a better correlation for the adsorption of MB on T-SLP at different

initial MB concentrations compared to the pseudo-first-order model. Similar kinetic results were also reported for the adsorption of dye onto other materials such as spent tea leaves (Hameed 2009), coconut shell (de Lima *et al*. 2012), and plantain peels (Garba *et al*. 2016). As can be seen from Fig. 7c, the regression was linear over the whole time range, but the plot did not pass through the origin, and this deviation from the origin or near saturation might be due to the difference in the mass transfer rate in the initial and final stages of adsorption. This phenomenon also suggests that adsorption involved intraparticle diffusion, but that was not the only rate-controlling step (Hameed 2009). From these results, it can be concluded that intraparticle diffusion is not the dominating mechanism for the adsorption of MB from aqueous solution by T-SLP. This finding is similar to that obtained in previous work on MB adsorption (Hameed *et al*. 2008b).

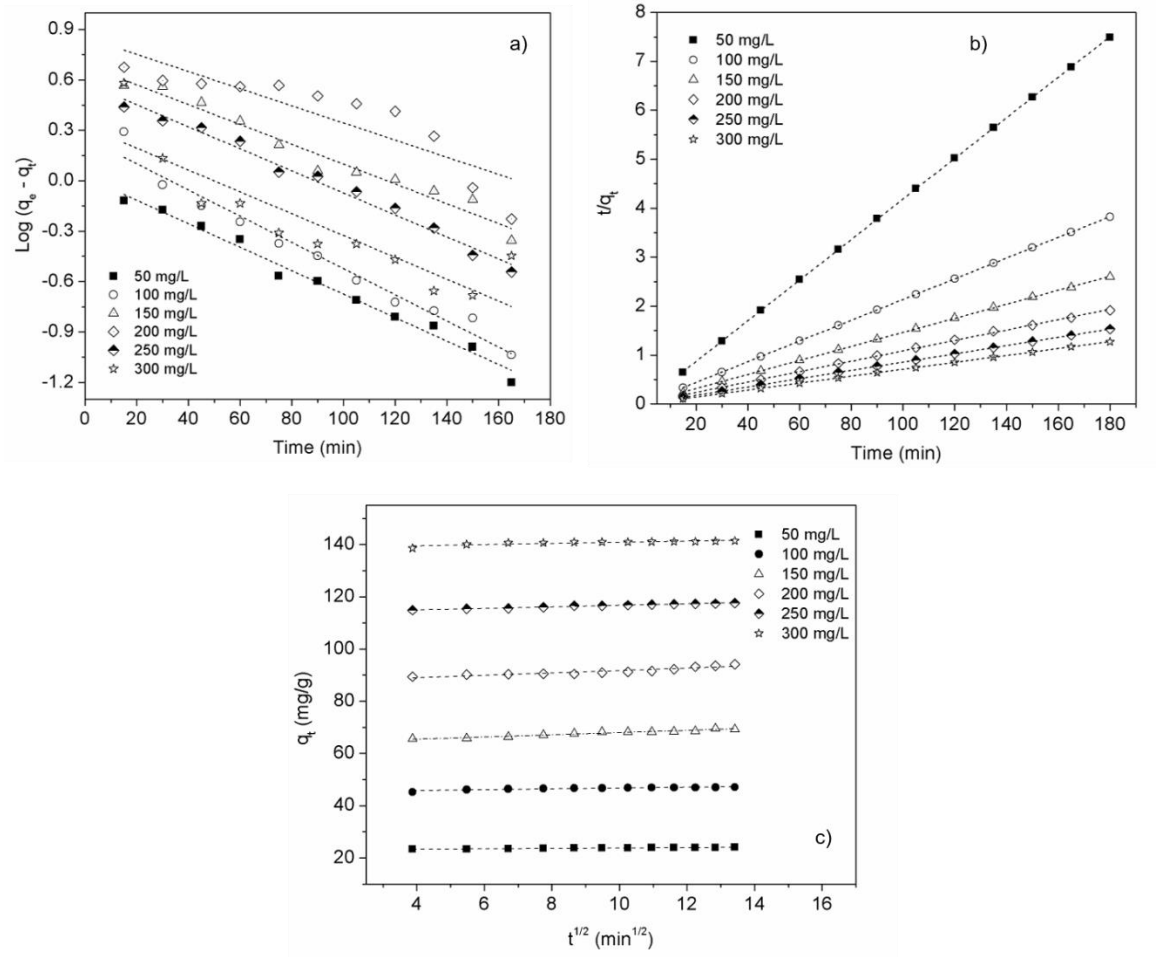

Fig. 7. a) Pseudo-first-order kinetics for adsorption of MB dye onto T-SLP; b) Pseudo-second-order kinetics for adsorption of MB dye onto T-SLP; c) Intraparticle diffusion plot for adsorption of MB dye onto T-SLP at different initial dye concentrations

CONCLUSIONS

1. This study showed that *Typha latifolia* powder possesses a high adsorption capacity and shows potential as an adsorbent for the removal of MB from aqueous solutions under optimized environmental conditions of adsorbent dose, pH, contact time, and initial dye concentrations.

2. The equilibrium data was well fitted by the Langmuir isotherm, and the maximum monolayer adsorption capacity of T-SLP was found to be 126.6 mg g^{-1}. The kinetics was well described by the pseudo-second-order model.
3. The maximum removal of 98.69% was obtained during the kinetic study in batch mode systems.
4. The adsorption capacity of T-SLP was found to be very competitive with the most recently reported adsorbents, with the additional advantages of low cost, easy availability of material, no required pretreatment step, and the potential to be applied as a complementary treatment in the tertiary treatment of wastewater.

ACKNOWLEDGMENTS

The financial support from the Mexican Science and Engineering Fair 2017, sponsored by the Council of Science and Technology of the State of Mexico (COMECYT) (Project No. 3912-2017), is gratefully acknowledged. The authors also thank the Technological Institute of Advanced Studies of Jocotitlan for providing instrumental support.

REFERENCES CITED

AlOthman, Z. A., Habila, M. A., Ali, R., Abdel Ghafar, A., and El-din Hassouna, M. S. (2014). "Valorization of two waste streams into activated carbon and studying its adsorption kinetics, equilibrium isotherms and thermodynamics for methylene blue removal," *Arab. J. Chem.* 7(6), 1148-1158. DOI: 10.1016/j.arabjc.2013.05.007

Anisuzzaman, S. M., Joseph, C. G., Krishnaiah, D., Bono, A., and Ooi, L. C. (2015). "Parametric and adsorption kinetic studies of methylene blue removal from simulated textile water using durian (*Durio zibethinus* Murray) skin," *Water Sci. Technol.* 72(6), 896-907. DOI: 10.2166/wst.2015.247

Chowdhury, S., Chakraborty, S., and Saha, P. (2011). "Biosorption of basic green 4 from aqueous solution by *Ananas comosus* (pineapple) leaf powder," *Colloids Surf. B: Biointerf.* 84(2), 520-527. DOI: 10.1016/j.colsurfb.2011.02.009

de Lima, A. C. A., Nascimento, R. F., de Sousa, F. F., Filho, J. M., and Oliveira, A. C. (2012). "Modified coconut shell fibers: A green and economical sorbent for the removal of anions from aqueous solutions," *Chem. Eng. J.* 185-186, 274-284 DOI: 10.1016/j.cej.2012.01.037

Dutta, S., Bhattacharyya, A., Ganguly, A., Gupta, S., and Basu, S. (2011). "Application of response surface methodology for preparation of low-cost adsorbent from citrus fruit peel and for removal of methylene blue," *Desalination* 275(1-3), 26-36. DOI: 10.1016/j.desal.2011.02.057

Esan, O. S., Abiola, O. N., Owoyomi, O., Aboluwoye, C. O., and Osundiya, M. O. (2014). "Adsorption of brilliant green onto luffa cylindrical sponge: Equilibrium, kinetics, and thermodynamic studies," *ISRN Phys. Chem.* 2014,743532. DOI: 10.1155/2014/743532

Etim, U. J., Umoren, S. A., and Eduok, U. M. (2016). "Coconut coir dust as a low cost adsorbent for the removal of cationic dye from aqueous solution," *J. Saudi Chem. Soc.* 20, S67-S76. DOI: 10.1016/j.jscs.2012.09.014

Garba, Z. N., Ugbaga, N. I., and Abdullahi, A. K. (2016). "Evaluation of optimum adsorption conditions for Ni(II) and Cd(II) removal from aqueous solution by modified plantain peels (MPP)," *Beni-Suef Univ. J. Basic Appl. Sci.* 5(2), 170-179. DOI: 10.1016/j.bjbas.2016.03.001

Gouamid, M., Ouahrani, M. R., and Bensaci, M. B. (2013). "Adsorption equilibrium, kinetics and thermodynamics of methylene blue from aqueous solutions using date palm leaves," *Energy Procedia* 36, 898-907. DOI: 10.1016/j.egypro.2013.07.103

Guo, J. Z., Li, B., Liu, L., and Lv, K. (2014). "Removal of methylene blue from aqueous solutions by chemically modified bamboo," *Chemosphere* 111, 225-231. DOI: 10.1016/j.chemosphere.2014.03.118

Hameed, B. H. (2009). "Spent tea leaves: A new non-conventional and low-cost adsorbent for removal of basic dye from aqueous solutions," *J. Hazard. Mater.* 161(2-3), 753-759. DOI: 10.1016/j.jhazmat.2008.04.019

Hameed, B. H., and Ahmad, A. A. (2009). "Batch adsorption of methylene blue from aqueous solution by garlic peel, an agricultural waste biomass," *J. Hazard. Mater.* 164(2-3), 870-875. DOI: 10.1016/j.jhazmat.2008.08.084

Hameed, B. H., and El-khaiary, M. I. (2008). "Sorption kinetics and isotherm studies of a cationic dye using agricultural waste: Broad bean peels," *J. Hazard. Mater.* 154(1-3), 639-648. DOI: 10.1016/j.jhazmat.2007.10.081

Hameed, B. H., Krishni, R. R., and Sata, S. A. (2009). "A novel agricultural waste adsorbent for the removal of cationic dye from aqueous solutions," *J. Hazard. Mater.* 162(1), 305-311. DOI: 10.1016/j.jhazmat.2008.05.036

Hameed, B. H., Mahmoud, D. K., and Ahmad, A. L. (2008a). "Equilibrium modeling and kinetic studies on the adsorption of basic dye by a low-cost adsorbent: Coconut (*Cocos nucifera*) bunch waste," *J. Hazard. Mater*. 158(1), 65-72. DOI: 10.1016/j.jhazmat.2008.01.034

Hameed, B. H., Mahmoud, D. K., and Ahmad, A. L. (2008b). "Sorption equilibrium and kinetics of basic dye from aqueous solution using banana stalk waste," *J. Hazard. Mater.* 158(2-3), 499-506. DOI: 10.1016/j.jhazmat.2008.01.098

Ho, Y. S., and McKay, G. (1999). "Pseudo-second order model for sorption processes", *Process Biochem.* 34(5), 451–65. DOI: 10.1016/S0032-9592(98)00112-5

Hu, Z., Chen, H., Ji, F., and Yuan, S. (2010). "Removal of congo red from aqueous solution by cattail root," *J. Hazard. Mater.* 173(1-3), 292-297. DOI: 10.1016/j.jhazmat.2009.08.082

Hubbe, M. A., Beck, K. R., O'Neal, G., and Sharma, Y. C. (2012). "Cellulosic substrates for removal of pollutants from aqueous systems: A review. 2. Dyes," *BioResources* 7(2), 2592-2687. DOI: 10.15376/biores.7.2.2592-2687

Irem, S., Mahmood Khan, Q., Islam, E., Jamal Hashmat, A., Anwar ul Haq, M., Afzal, M., and Mustafa, T. (2013). "Enhanced removal of reactive navy blue dye using powdered orange waste," *Ecol. Eng.* 58, 399-405. DOI: 10.1016/j.ecoleng.2013.07.005

Kumari, M., and Tripathi, B. D. (2015). "Efficiency of *Phragmites australis* and *Typha latifolia* for heavy metal removal from wastewater," *Ecotoxicol. Environ. Saf.* 112, 80-86. DOI: 10.1016/j.ecoenv.2014.10.034

Lagergren, S. (1898). "About the theory of so-called adsorption of soluble substances", *Kung Sven. Veten. Hand.* 24(4), 1–39.

Lu, Y., and Liang, Q. (2013). "Removal of Pb(II) from vanillin solution by acid-modified cattail biomass," *BioResources* 8(2), 2631-2640. DOI: 10.15376/biores.8.2.2631-2640

Meng, H., Wang, X., Tong, S., Lu, X., Hao, M., An, Y., and Zhang, Z. (2016). "Seed germination environments of *Typha latifolia* and *Phragmites australis* in wetland restoration," *Ecol. Eng.* 96, 194-199. DOI: 10.1016/j.ecoleng.2016.03.003

Nasuha, N., and Hameed, B. H. (2011). "Adsorption of methylene blue from aqueous solution onto NaOH-modified rejected tea," *Chem. Eng. J.* 166(2), 783-786. DOI: 10.1016/j.cej.2010.11.012.

Peydayesh, M., and Rahbar-Kelishami, A. (2015). "Adsorption of methylene blue onto *Platanus orientalis* leaf powder: Kinetic, equilibrium and thermodynamic studies," *J. Ind. Eng. Chem*. 21, 1014-1019. DOI: 10.1016/j.jiec.2014.05.010

Rebaque, D., Martínez-Rubio, R., Fornalé, S., García-Angulo, P., Alonso-Simón, A., Álvarez, J. M., Caparros-Ruiz, D., Acebes, J. L., and Encina, A. (2017). "Characterization of structural cell wall polysaccharides in cattail (*Typha latifolia*): Evaluation as potential biofuel feedstock," *Carbohydr. Polym.* 175, 679-688 DOI: 10.1016/j.carbpol.2017.08.021

Rodriguez-Hernandez, M. C., Garcia De la-Cruz, R. F., Leyva, E., and Navarro-Tovar, G. (2017). "*Typha latifolia* as potential phytoremediator of 2,4-dichlorophenol: Analysis of tolerance, uptake and possible transformation processes," *Chemosphere* 173, 190-198. DOI: 10.1016/j.chemosphere.2016.12.043

Saif Ur Rehman, M., and Han, J. I. (2013). "Biosorption of methylene blue from aqueous solutions by *Typha angustata* phytomass," *Int. J. Environ. Sci. Technol.* 10(4), 865-870. DOI: 10.1007/s13762-012-0128-5

Saif, M., Rehman, U., Kim, I., and Han, J. (2012). "Adsorption of methylene blue dye from aqueous solution by sugar extracted spent rice biomass," *Carbohydr. Polym.* 90(3), 1314-1322. DOI: 10.1016/j.carbpol.2012.06.078

Shakoor, S., and Nasar, A. (2016). "Removal of methylene blue dye from artificially contaminated water using *Citrus limetta* peel waste as a very low cost adsorbent," *J. Taiwan Inst. Chem. Eng.* 66, 154-163. DOI: 10.1016/j.jtice.2016.06.009

Shi, Q., Zhang, J., Zhang, C., Li, C., Zhang, B., Hu, W., Xu, J., and Zhao, R. (2010). "Preparation of activated carbon from cattail and its application for dyes removal," *J. Environ. Sci.* 22(1), 91-97. DOI: 10.1016/S1001-0742(09)60079-6

Weber, W. J., and Morris, J. C. (1963). "Kinetics of adsorption on carbon from solution", *J. Sanit. Eng. Div. ASCE*, 89(2), 31–60.

Xu, W., Shi, W., Yan, F., Zhang, B., and Liang, J. (2011). Mechanisms of cadmium detoxification in cattail (*Typha angustifolia* L.). *Aquat. Bot*. 94, 37–43. DOI: 10.1016/j.aquabot.2010.11.002

Zhou, Q., Gong, W. Q., Li, Y. B., Chen, S. H., Yang, D. J., Bai, C. P., Liu, X. F., and Xu, N. (2011). "Biosorption of methylene blue onto spent corncob substrate: Kinetics, equilibrium and thermodynamic studies," *Water Sci. Technol.* 63(12), 2775-2780. DOI: 10.2166/wst.2011.542

Article submitted: October 1, 2017; Peer review completed: December 29, 2017; Revised version received: Jan. 11, 2018; Accepted: Jan. 13, 2018; Published: Jan. 22, 2018.
DOI: 10.15376/biores.13.1.1696-1710